Molecular and environmental cues in cardiac differentiation of mesenchymal stem cells

Ramkisoensing, A.A.

CHAPTER IV

GAP JUNCTIONAL COUPLING WITH CARDIOMYOCYTES IS ESSENTIAL FOR CARDIOMYOGENIC DIFFERENTIATION OF FETAL HUMAN MESENCHYMAL STEM CELLS

Arti A. Ramkisoensing[a], *Daniël A. Pijnappels*[a], *Jim Swildens*[a,b], *Marie José Goumans*[b], *Willem E. Fibbe*[c], *Martin J. Schalij*[a], *Antoine A.F. de Vries*[a,b]*, *Douwe E. Atsma*[a]*
**Equal contribution*

[a]Departments of Cardiology, [b]Molecular Cell Biology, [c]Hematology, Laboratory of Experimental Cardiology, Leiden University Medical Center, 2300 RC Leiden, The Netherlands.

Stem Cells. 2012 Jun;30(6):1236-45.

ABSTRACT

Rationale: Gap junctional coupling is important for functional integration of transplanted cells with host myocardium. However, the role of gap junctions in cardiomyogenic differentiation of transplanted cells has not been directly investigated.

Objective: To study the role of connexin43 (Cx43) in cardiomyogenic differentiation of human mesenchymal stem cells (hMSCs).

Methods: Knockdown of Cx43 gene expression was established in naturally Cx43-rich fetal amniotic membrane hMSCs (Cx43↓ fetal AM hMSCs), while Cx43 was overexpressed in inherently Cx43-poor adult adipose tissue hMSCs (Cx43↑ adult AT hMSCs). The hMSCs were exposed to cardiomyogenic stimuli by co-incubation with neonatal rat cardiomyocytes (nrCMCs) for 10 days. Differentiation was assessed by immunostaining and whole-cell current-clamping. To establish whether the effects of Cx43 knockdown could be rescued Cx45 was overexpressed in Cx43↓ fetal AM hMSCs.

Results: Ten days after co-incubation not a single Cx43↓ fetal AM hMSC or adult AT MSC expressed α-actinin, while control fetal AM hMSCs did (2.18±0.4%, n=5,000). Moreover, functional cardiomyogenic differentiation, based on action potential recordings, occurred only in control fetal AM hMSCs. Of interest, Cx45 overexpression in Cx43↓ fetal AM hMSCs restored their ability to undergo cardiomyogenesis (1.57±0.4%, n=2,500) in co-culture with nrCMCs.

Conclusion: Gap junctional coupling is required for differentiation of fetal AM hMSCs into functional cardiomyocytes after co-incubation with nrCMCs. Heterocellular gap junctional coupling thus plays an important role in the transfer of cardiomyogenic signals from nrCMCs to fetal hMSCs but is not sufficient to induce cardiomyogenic differentiation in adult AT hMSCs.

INTRODUCTION

Gap junctional coupling is essential in establishing electrochemical communication between cardiomyocytes (CMCs).[1] Such coupling of cytoplasmic compartments is mediated by gap junctions, consisting of two hexameric assemblies of connexin (Cx) proteins embedded in the plasma membranes of neighboring cells thereby forming so-called hemichannels or connexons. Gap junctions permit the bidirectional passage of small molecules and ions between cells and play an important role in the regulation of both physiological and pathophysiological processes.

During embryonic development, spreading of signals across tissues through gap junctions contribute to the migration and specialization of cells.[2] In the developing heart, connexin40 (Cx40), connexin43 (Cx43) and/or connexin45 (Cx45) deficiency results in serious cardiac malformation.[3-7] Besides cardiac development, gap junctional communication also affects the therapeutic and hazardous potential of cardiac cell therapy.[8-10] However, the role of gap junctional coupling in cardiomyogenic differentiation of stem cells remains unclear, although gap junction-mediated processes, such as spread of micro RNAs (miRs) and hyperpolarization, have been implicated in the induction of cardiomyogenesis.[11,12]

Mesenchymal stem cells (MSCs) are a population of mononuclear stromal cells that can be harvested from a wide variety of tissues, are easily expandable *in vitro*, have immunomodulatory properties, secrete paracrine factors that stimulate tissue regeneration and can differentiate into various types of mesodermal and non-mesodermal cells.[13,14] In addition, these cells were shown to improve cardiac function upon transplantation in diseased rodent, pig and human hearts.[15] However, to what extent MSCs can undergo cardiac differentiation and which factors are involved in this process is still unclear.[16-18] Although donor age and heterocellular interactions were found to affect the cardiomyogenic differentiation potential of MSCs[19], more research is needed into their biological properties and the modification thereof to improve the therapeutic potential of MSC-based cardiac cell therapy.

Accordingly, in this study, we specifically investigated the role of Cx43, the major gap junction protein of the working myocardium, in cardiomyogenic differentiation of naturally Cx43-rich fetal and Cx43-poor adult human MSCs (hMSCs)[19] in cocultures with neonatal rat ventricular CMCs (nrCMCs). To this end, Cx43 expression levels in hMSCs were either downregulated by short hairpin RNA (shRNA)-mediated RNA interference (RNAi) or upregulated by recombinant human Cx43 (hCx43) gene delivery. To control for possible off-target effects of hCx43-specific shRNAs, an RNAi rescue experiment based on the forced expression of human Cx45 (hCx45) in Cx43 knockdown cells was included. The consequences of these genetic interventions on the cardiomyogenic differentiation capacity of the hMSCs were assessed using immunocytological and patch-clamp analyses.

The present study shows that gap junctions are directly involved in the transfer of cardiomyogenic signals from nrCMCs to fetal hMSCs. Downregulation of Cx43 gene expression in these hMSCs prevented their cardiomyogenic differentiation in co-cultures with nrCMCs. Overexpression of hCx45 in the Cx43 knockdown cells, on the other hand, restored their ability to respond to cardiomyogenic stimuli provided by neighboring nrCMCs.

MATERIALS AND METHODS

The role of gap junctional coupling in the transfer of cardiomyogenic signals from nrCMCs to hMSCs was investigated by suppressing Cx43 expression in naturally Cx43-rich fetal amniotic membrane (AM) hMSCs using two lentiviral vectors (LVs) encoding different hCx43-specific shRNAs (Cx43↓(1) fetal AM hMSCs and (Cx43↓(2) fetal AM hMSCs) and by LV-mediated overexpression of hCx43 in intrinsically Cx43-poor adult adipose tissue (AT) hMSCs (Cx43↑ adult AT hMSCs). To facilitate the identification of genetically modified cells, the LVs also directed the synthesis of the green fluorescent protein (GFP) of *Renilla reniformis* (hrGFP). Fetal AM hMSCs transduced with an LV encoding an shRNA directed against the *Aequorea victoria* enhanced green fluorescent protein (eGFP) gene and adult AT hMSCs transduced with an LV coding for hrGFP alone served as control cells (control fetal AM hMSCs and control adult AT hMSCs, respectively). For an optimized analysis of the adult AT hMSCs these cells were also transduced with an LV encoding Cx43 and a puromycin resistence gene. Control cells were transduced with an LV coding for the puromycin-resistence gene alone. Immunocytological analysis, quantitative reverse transcriptase-polymerase chain reaction (qRT-PCR) and western blot analysis were applied to determine Cx43 expression levels, while dye transfer assays and whole-cell current-clamp recordings were used to assess the level of functional coupling. To induce cardiomyogenic differentiation, hMSCs were co-incubated with nrCMCs for 10 days. Differentiation was assessed by immunocytological staining and whole-cell current-clamping. LV-encoded hCx45 was overexpressed in Cx43↓(1) fetal AM hMSCs (Cx43↓(1)+Cx45↑ fetal AM hMSCs) to establish whether the effects of Cx43 knockdown could be reversed using the techniques described above. Cx43↓(1) fetal AM hMSCs transduced with an LV encoding eGFP were used as control cells (Cx43↓(1)+eGFP fetal AM hMSCs) in these experiments. For a detailed description of the materials and methods the reader is referred to the Supplement Material and previous papers of our research group.[19-21]

RESULTS

CHARACTERIZATION OF FETAL AM HMSCS AND ADULT AT HMSCS

Both fetal AM hMSCs and adult AT hMSCs were characterized according to established criteria. To this purpose, their cell surface marker profile and adipogenic and osteogenic differentiation capacity were studied. Both types of hMSCs were negative for CD31 (endothelial cell marker), CD34 and CD45 (both hematopoietic cell markers), whereas they were positive for CD73, CD90 and CD105 (mesenchymal stem cell markers) (Figure 1A-C). *In vitro* differentiation assays showed that the two types of hMSCs were able to differentiate into adipocytes (Figure 1D1-D2) and osteoblasts (Figure 1E1-E2) confirming their multipotency.

EVALUATION OF CX43 EXPRESSION LEVELS

The impact of the different genetic interventions on the Cx43 expression levels in fetal AM hMSCs and adult AT hMSCs was investigated by three different methods. Immunocytological analysis showed that Cx43↑ adult AT hMSCs (Figure 2A2) contained higher levels of Cx43 than control adult AT hMSCs (Figure 2A1), while the protein was also more abundant in control fetal AM hMSCs (Figure 2B1) than in Cx43↓(1) fetal AM hMSCs (Figure 2B2) or in Cx43↓(2) fetal AM hMSCs (Figure 2B3) (for each genetic modification n=4 isolates of each hMSC type were assessed). These results were validated by western blot analysis (n=4 hMSC isolates per experimental group), which showed that Cx43↑ adult AT hMSCs contained 1,798±146% more Cx43 protein than control adult AT hMSCs ($P<0.001$) (Figure 2C1 and C3). Western blot analysis also confirmed the presence of significantly less Cx43 in Cx43↓(1) fetal AM hMSCs (79.4±3.0% reduction) and in Cx43↓(2) fetal AM hMSCs (77.4±2.6% reduction) than in control fetal AM hMSCs ($P<0.001$) (Figure 2C2 and C4). In agreement with these results, qRT-PCR revealed that Cx43↑ adult AT hMSCs contained 9.77±0.63-fold ($P<0.001$) (Figure 2D1) more Cx43 transcripts than control adult AT hMSCs while the amount of Cx43 RNA in Cx43↓(1) fetal AM hMSCs and in Cx43↓(2) fetal AM hMSCs was, respectively, 3.67±0.14- and 3.94±0.25-fold ($P<0.001$) lower than in control fetal AM hMSCs (Figure 2D2).

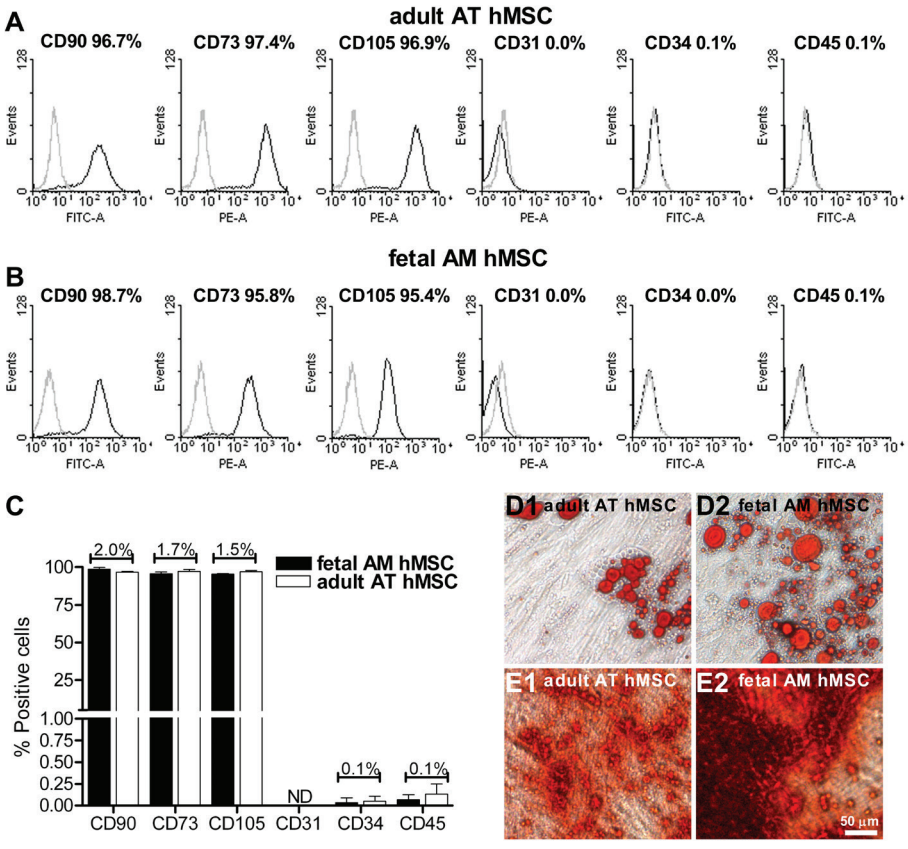

Figure 1. Characterization of fetal AM hMSCs and adult AT hMSCs. (A-B) Flow cytometric analyses showed for both types of hMSCs abundant surface expression of the MSC markers, CD90, CD105 and CD73 and hardly any surface expression of the hematopoietic cell markers CD34 and CD45 or the endothelial cell marker CD31 (black lines). Isotype-matched control antibodies were included to determine background fluorescence levels (gray lines). Percentages are means of ≥4 measurements. (C) Only minor differences in the expression levels of the surface marker proteins were present between fetal AM hMSCs and adult AT hMSCs. ND is not detected. (D1-D2) Adipogenic differentiation was visualized by the presence of Oil Red O-stained fat vacuoles. (E1-E2) Calcium depositions after osteogenic differentiation were visualized by Alizarin Red S staining.

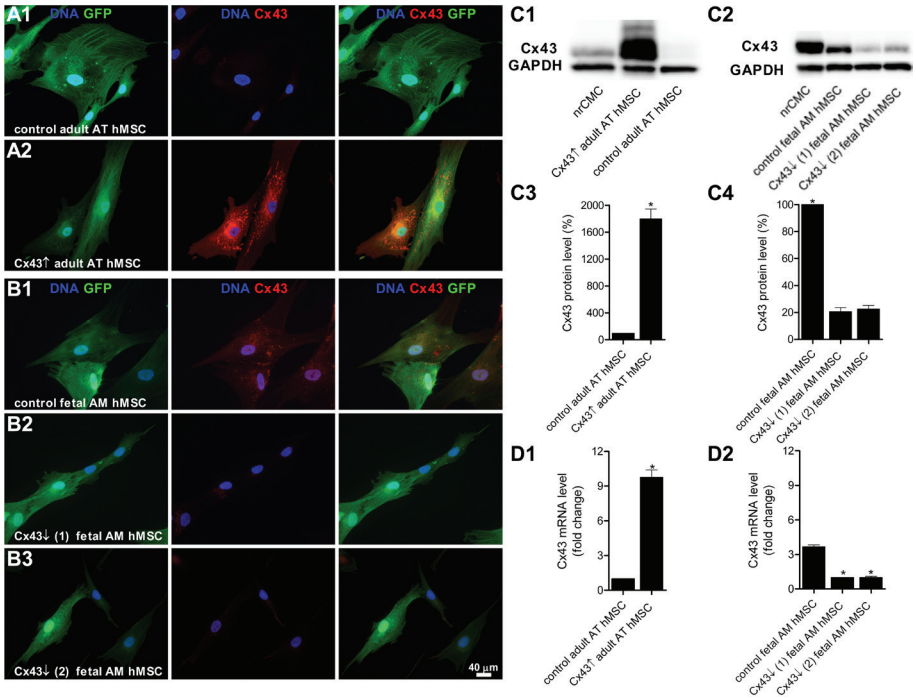

Figure 2. Analysis by immunofluorescence microscopy, western blotting and qRT-PCR of Cx43 expression in monocultures of genetically modified fetal AM hMSCs and adult AT hMSCs. (A1-A2) Immunocytological analyses revealed low Cx43 levels in control adult AT hMSCs, while high levels of Cx43 were detected in Cx43↑ adult AT hMSCs. (B1) High Cx43 levels were present in control fetal AM hMSCs. (B2-B3) After knockdown of Cx43 gene expression, low Cx43 levels were detected in Cx43↓(1) fetal AM hMSCs and in Cx43↓(2) fetal AM hMSCs. Nuclei were stained with the DNA-binding fluorochrome Hoechst 33342. (C1-C2) Pictures of representative western blots showing that Cx43↑ adult AT hMSCs have large amounts of Cx43 in contrast to control adult AT hMSCs and that control fetal AM hMSCs contain large amounts of Cx43 in contrast to Cx43↓(1) fetal AM hMSCs and Cx43↓(2) fetal AM hMSCs. The GAPDH-specific immunostaining was included for normalization purposes. (C3-C4) Bar graphs of the quantification by western blotting of Cx43 levels in the different populations of hMSCs corrected for differences in GAPDH expression. *P<0.001 vs. Cx43↑ adult AT hMSCs or vs. Cx43↓(1) fetal AM hMSCs and Cx43↓(2) fetal AM hMSCs. (D1-D2) Bar graphs of the assessment by qRT-PCR of Cx43 mRNA levels in control adult AT hMSCs, Cx43↑ adult AT hMSCs and in control fetal AM hMSCs, Cx43↓(1) fetal AM hMSCs and Cx43↓(2) fetal AM hMSCs. *P<0.001 vs. control adult AT hMSCs or vs. Cx43↓(1) fetal AM hMSCs and Cx43↓(2) fetal AM hMSCs.

ASSESSMENT OF FUNCTIONAL HETEROCELLULAR GAP JUNCTIONAL COUPLING VIA CX43

The effects of modulating Cx43 expression levels in fetal AM hMSCs and in adult AT hMSCs on their functional heterocellular coupling with nrCMCs were investigated by dye transfer experiments using the gap junction-permeable fluorochrome calcein red-orange AM (calcein). Cx43↑ adult AT hMSCs showed a significantly higher dye intensity than control adult AT hMSCs (67.6±4.7% vs. 8.43±1.6% of that in adjacent nrCMCs) (P<0.001) (Figure 3A1-A2 and C1). Furthermore, the fraction of hMSCs that took up calcein from neighboring nrCMCs was much higher for the Cx43↑ adult AT hMSCs than for the control adult AT hMSCs (71.6±7.6% vs. 28.3±4.6% of cells) (P<0.001) (Figure 3C3). The relative dye intensity in control fetal AM hMSCs (63.2±3.8%) was higher than in Cx43↓(1) fetal AM hMSCs (5.94±1.4%) and in Cx43↓(2) fetal AM hMSCs (6.00±1.9%) (P<0.001) (Figure 3B1-B3 and C2). Moreover, significantly more of the control fetal AM hMSCs (75.9±9.2%) had taken up calcein than of the Cx43↓(1) fetal AM hMSCs (13.2±2.4%) or of the Cx43↓(2) fetal AM hMSCs (13.0±2.1%) (P<0.001) (Figure 3C4).

To further assess functional coupling between hMSCs and nrCMCs, maximal diastolic membrane potentials (MDPs) were measured in each group of hMSCs in the absence and presence of adjacent nrCMCs. Similar average MDPs were found in hMSC monocultures (n=6) (Figure 3D, black bars). However, MDPs, on average, became more negative when nrCMCs were adjoining the hMSCs, although the degree of hyperpolarization differed between the various groups (n=8) (Figure 3D, white bars). Cx43↑ adult AT hMSCs and control fetal AM hMSCs showed the most negative MDPs (-38±4 mV and -43±5 mV, respectively). On the other hand, control adult AT hMSCs, Cx43↓(1) fetal AM hMSCs and Cx43↓(2) fetal AM hMSCs, which all contain low levels of Cx43, showed less negative MDPs.

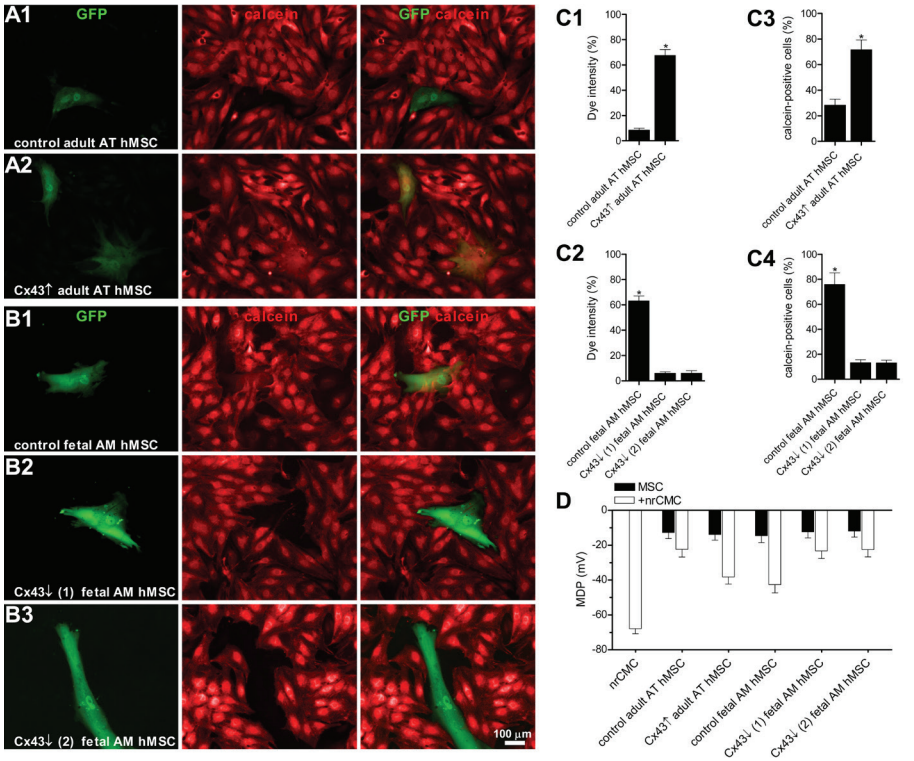

Figure 3. Study of the influence of Cx43 levels in hMSCs on their functional coupling with nrCMCs. (A1-A2) Calcein transfer from nrCMCs to Cx43↑ adult AT hMSCs was much more efficient than to control adult AT hMSCs. (B1-B3) Dye transfer from nrCMCs to fetal AM hMSCs was strongly inhibited by shRNA-mediated downregulation of Cx43 gene expression in the hMSCs. (C1-C2) Bar graphs of the quantification of dye intensity in GFP-positive hMSCs. Dye intensity in the GFP-positive hMSCs was expressed as percentage of the dye intensity in the surrounding nrCMCs. (C3-C4) Bar graphs of the assessment of the percentage of GFP-positive hMSCs that had taken up calcein from neighboring nrCMCs. *P<0.001 vs. control adult AT hMSC or vs. Cx43↓(1) fetal AM hMSCs and Cx43↓(2) fetal AM hMSCs. (D) Average MDPs in hMSC monocultures (indicated as MSC) as measured by whole-cell current-clamping were similar for the different experimental groups. However, the average MDP in hMSCs became more negative in the presence of adjoining nrCMCs (indicated as MSC-CMC), with Cx43↑ adult AT hMSCs and control fetal AM hMSCs reaching the most negative values.

ASSESSMENT OF CARDIOMYOGENIC DIFFERENTIATION ABILITY OF HMSCS WITH GENETICALLY ALTERED CX43 LEVELS

Human-specific immunocytological evaluation

At day 10 of co-culture with nrCMCs, 2.27±0.4% GFP/human lamin A/C-double-positive control fetal AM hMSCs were positive for the sarcomeric protein α-actinin with a cross-striated staining pattern like that of the nrCMCs (Figure 4A1-A2 and C). However, GFP/human lamin A/C-double-positive Cx43↓(1) fetal AM hMSCs and Cx43↓(2) fetal AM hMSCs did not contain detectable amounts α-actinin (Figure 4A3-A4 and C). Furthermore, neither Cx43↑ adult AT hMSCs nor control adult AT hMSCs stained positive for α-actinin (Figure 4B1-B3 and C). These results were confirmed with Cx43↑ adult AT hMSCs and control adult AT hMSCs that were transduced with LVs that encoded the puromycin-resistence gene instead of GFP (Supplemental figure 1A – B). Also, only in co-cultures of control fetal AM hMSCs with nrCMCs, some GFP-positive cells were detected to be positive for the cardiac transcription factors Nkx2.5 and GATA4 (Supplemental figure 2A1 and 3A1). In the other hMSC groups, all GFP-positive cells were negative for these cardiac transcription factors (Supplemental figure 2A2-B2 and 3A2-B2).

hMSC-specific intracellular electrophysiological measurements

To assess cardiomyogenic differentiation at a functional level, the ability of GFP-positive hMSCs to generate spontaneous action potentials was studied after gap junction uncoupling (Figure 5A-B). A fraction of the control fetal AM hMSCs showed spontaneous action potentials (n=6), with MDPs similar to those of native CMCs (n=9) (Figure 5B-C). In contrast, both Cx43↑ adult AT hMSCs and control adult AT hMSCs (n=7) showed more depolarized MDPs of -15.0±4 mV and -14.8±3 mV, respectively. Also, Cx43↑ adult AT hMSCs stayed inexcitable (n=5). Importantly, knockdown of Cx43 in fetal AM hMSCs rendered these cells incapable of generating spontaneous action potentials after 10 days of co-culture with nrCMCs (n=9 for both shRNAs) and left them with an MDP comparable to those of adult AT hMSCs (-15 mV vs. -12 and -14 mV for Cx43↓(1) fetal AM hMSCs and for Cx43↓(2) fetal AM hMSCs, respectively).

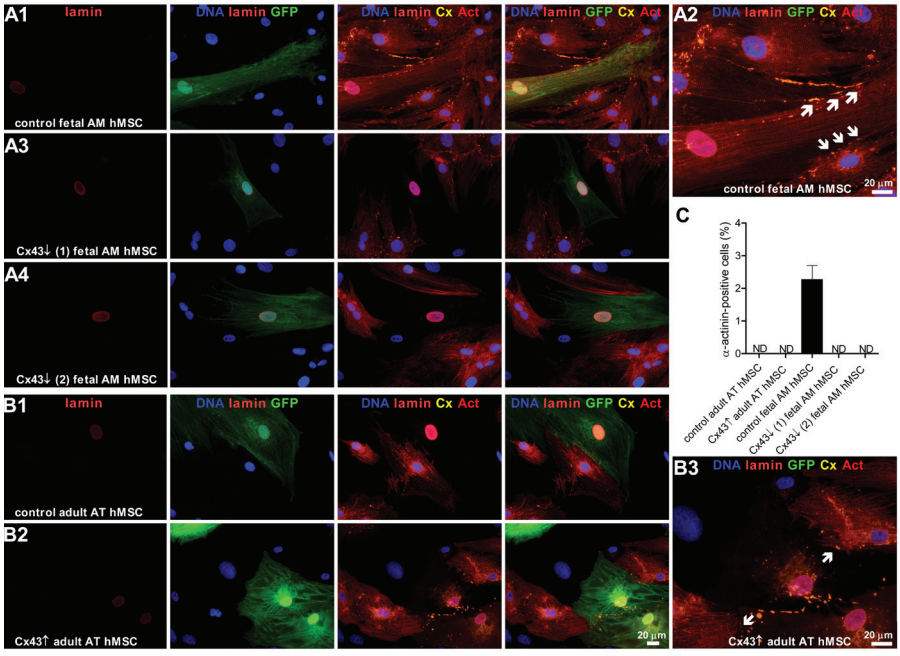

Figure 4. Immunocytological assessment of cardiomyogenic differentiation of genetically modified adult AT hMSCs and fetal AM hMSCs after 10 days of co-culture with nrCMCs. (A1) Upon co-culture with nrCMCs, a fraction of the GFP- and human lamin A/C-double-positive control fetal AM hMSCs became positive for sarcomeric α-actinin (indicated as Act). (A2) Intense punctate Cx43 (indicated as Cx) immunostaining of the interfaces between a control fetal AM hMSC and two adjacent nrCMCs (white arrows). (A3-A4, B1-B2) GFP-labeled Cx43↓(1) fetal AM hMSCs, Cx43↓(2) fetal AM hMSCs, Cx43↑ adult AT hMSCs and control adult AT hMSCs in co-culture with nrCMCs did not stain positive for α-actinin. (B3) Presence of Cx43 plaques at the interfaces between Cx43↑ adult AT hMSCs and two bordering nrCMCs (white arrows). (C) Quantitative analysis of the cardiomyogenic differentiation ability of the genetically modified hMSCs using immunopositivity for sarcomeric α-actinin as read-out. The graph is based on a minimum of 5,000 cells analyzed from 4 separate hMSC isolates per experimental group. ND is not detected.

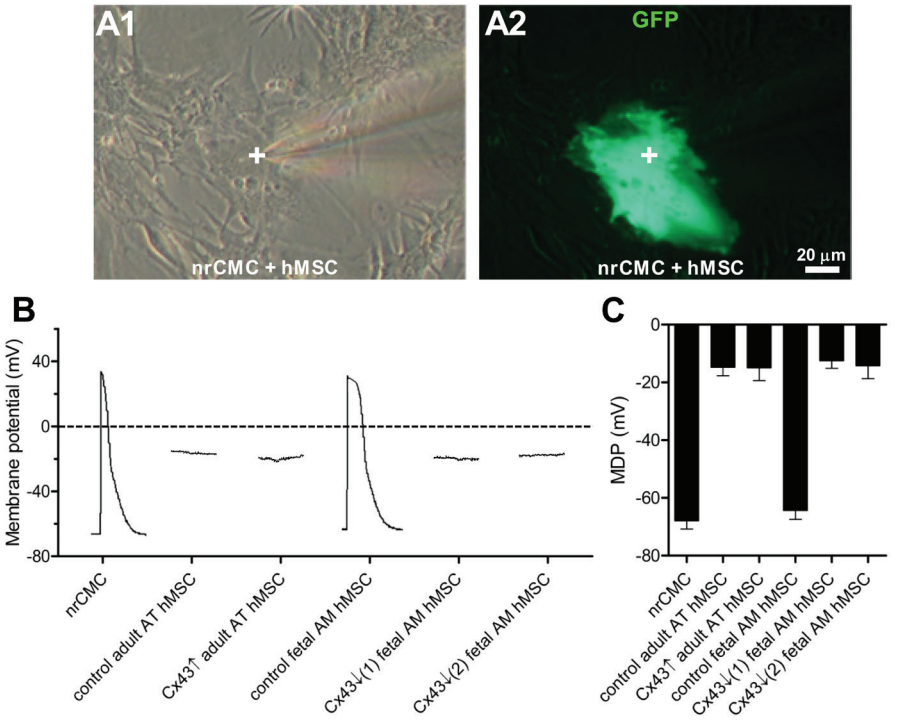

Figure 5. Electrophysiological assessment, after gap junctional uncoupling, of cardiomyogenic differentiation of hMSCs. (A1-A2) Bright field (A1) and fluorescence (A2) image of a GFP-positive hMSC with adjacent nrCMCs and patch-clamp electrode. (B) Current-clamp recordings in nrCMCs and in GFP-positive hMSCs from the different experimental groups. Action potentials were measured in nrCMCs and in some control fetal AM hMSCs, while the other cells displayed stable membrane potentials. (C) Average MDPs of nrCMCs and in the different groups of GFP-positive hMSCs. For the control fetal AM hMSCs, only the average MDP of cells showing action potentials is presented.

EVALUATION OF CX45 EXPRESSION LEVELS

To check whether the inability of Cx43↓ fetal AM hMSCs to undergo cardiomyogenic differentiation in co-cultures with nrCMCs was not caused by some off-target effect(s) of the hCx43-specific shRNAs, a rescue experiment was carried out. To this end, the Cx43↓(1) fetal AM hMSCs were transduced with an LV encoding hCx45 or with a control LV directing the synthesis of eGFP. Immunocytological analysis of the resulting cell populations showed that Cx45 was much more abundant in Cx43↓(1)+Cx45↑ fetal AM hMSCs than in Cx43↓(1)+eGFP fetal AM hMSCs (Figure 6A1-A2). Western blot analysis confirmed these results by showing 1,163±57% higher levels of Cx45 in Cx43↓(1)+Cx45↑ fetal AM hMSCs than in Cx43↓(1)+eGFP fetal AM hMSCs (n=4 for both sample types) (P<0.001) (Figure 6B1-B2). Consistently, qRT-PCR showed that Cx45 transcript levels were 12.5±1.9 fold higher in Cx43↓(1)+Cx45↑ fetal AM hMSCs than in Cx43↓(1)+eGFP fetal AM hMSCs (P<0.01) (Figure 6C).

ASSESSMENT OF FUNCTIONAL HETEROCELLULAR GAP JUNCTIONAL COUPLING VIA CX45

The extent of functional heterocellular coupling between nrCMCs and Cx43↓(1)+Cx45↑ fetal AM hMSCs or Cx43↓(1)+eGFP fetal AM hMSCs was determined in dye transfer assays. The dye intensity relative to that in neighboring nrCMCs was much higher in Cx43↓(1)+Cx45↑ fetal AM hMSCs (92.3±3.2%) than in Cx43↓(1)+eGFP fetal AM hMSCs (5.96±0.8%) (P<0.001) (Figure 6D1-D2 and E1). Also, the proportion of hMSCs that took up calcein from adjacent nrCMCs was ~4-fold higher for the Cx43↓(1)+Cx45↑ fetal AM hMSCs than for the Cx43↓(1)+eGFP fetal AM hMSCs (66.7±7.6% vs. 16.0±2.3%) (P<0.001) (Figure 6E2).

To study the impact of Cx45 overexpression on the electrophysiological properties of Cx43↓ fetal AM hMSCs, whole-cell current-clamp measurements were performed. Cx45 overexpression did not significantly alter the average MDP of Cx43↓(1) fetal AM hMSCs in monoculture (n=6) (Figure 6F). However, in co-culture with nrCMCs, Cx43↓(1)+Cx45↑ fetal AM hMSCs (n=6) showed more negative MDPs as compared to Cx43↓(1)+eGFP fetal AM hMSCs (-24.8±5 mV and -43±5 mV, respectively) (Figure 6F), indicating that electrical coupling of Cx43↓ fetal AM hMSCs with neighboring nrCMCs was enhanced by Cx45 overexpression.

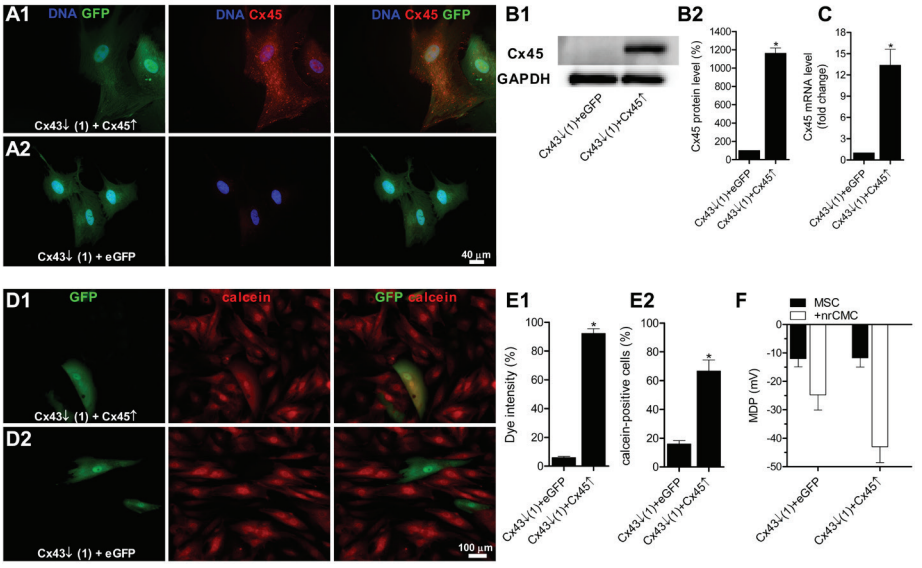

Figure 6. Assessment of Cx45 expression and functionality. (A1-A2) Immunocytological analyses showed abundant Cx45 expression in monocultures of Cx43↓(1)+Cx45↑ fetal AM hMSCs but not of Cx43↓(1)+eGFP fetal AM hMSCs. A part of the Cx45 signal was detected at the interfaces between Cx43↓(1)+Cx45↑ fetal AM hMSCs. Nuclei were stained with Hoechst 33342. (B1) Representative picture of a western blot confirming high-level expression of Cx45 in Cx43↓(1)+Cx45↑ fetal AM hMSCs and the presence of very low amounts of Cx45 in Cx43↓(1)+eGFP fetal AM hMSCs. The GAPDH-specific immunostaining was included for normalization purposes. (B2) Bar graph of the assessment by western blotting of Cx45 levels in Cx43↓(1)+Cx45↑ fetal AM hMSCs and in Cx43↓(1)+eGFP fetal AM hMSCs corrected for differences in GAPDH expression. *P<0.001 vs. Cx43↓(1)+eGFP fetal AM hMSCs. (C) Bar graph of the quantification by qRT-PCR of Cx45 mRNA levels in Cx43↓(1)+Cx45↑ fetal AM hMSCs and in Cx43↓(1)+eGFP fetal AM hMSCs. *P<0.01 vs. Cx43↓(1)+eGFP fetal AM hMSCs. (D1-D2) Cx43↓(1)+Cx45↑ fetal AM hMSCs much more readily take up calcein from adjacent nrCMCs than Cx43↓(1)+eGFP fetal AM hMSCs. (E1) Quantitative analysis of the dye intensity in Cx43↓(1)+Cx45↑ fetal AM hMSCs and in Cx43↓(1)+eGFP fetal AM hMSCs. Dye intensity in GFP-positive hMSCs was expressed as percentage of the dye intensity in the surrounding nrCMCs. (E2) Bar graph of the assessment of the percentage GFP-positive hMSCs that had taken up calcein from neighboring nrCMCs. *P<0.001 vs. Cx43↓(1)+eGFP fetal AM hMSCs. (F) The average MDPs of Cx43↓(1)+Cx45↑ fetal AM hMSCs and of Cx43↓(1)+eGFP fetal AM hMSCs in monocultures are less negative than in co-cultures with nrCMCs. The effect of adjacent nrCMCs on the average MDP was bigger for fetal AM hMSCs in which the knockdown of Cx43 expression was compensated by Cx45 overexpression than for Cx43↓(1)+eGFP fetal AM hMSCs.

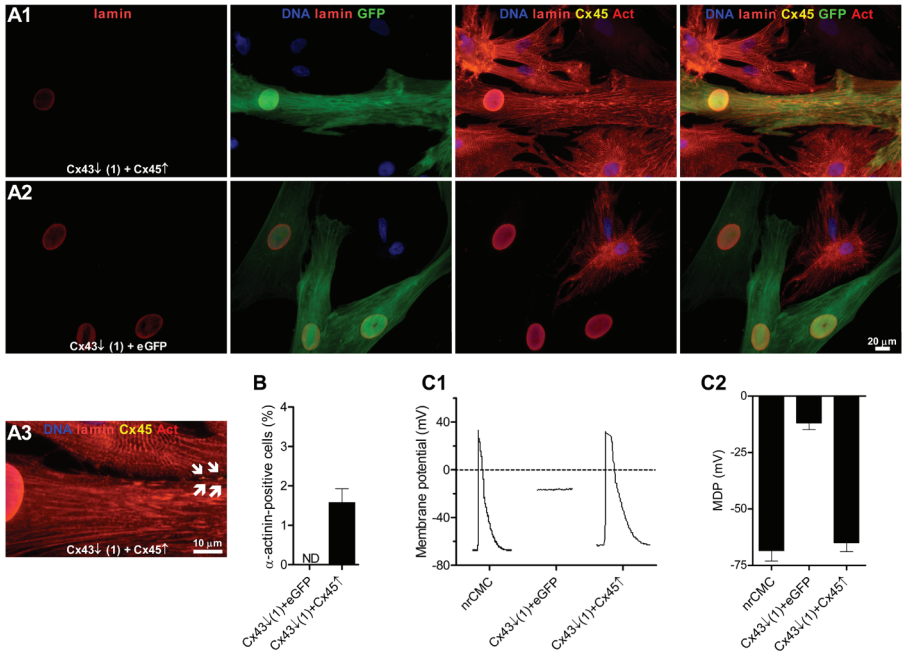

Figure 7. Investigation by immunocytological and patch-clamp analysis of cardiomyogenic differentiation of fetal AM hMSCs in co-culture with nrCMCs after rescue of Cx43 knockdown by Cx45 overexpression. In the presence of nrCMCs, a fraction of the GFP- and human lamin A/C-double-positive Cx43↓(1)+Cx45↑ fetal AM hMSCs (A1) expressed α-actinin (indicated as Act) in a striated pattern typical of sarcomeric proteins, while Cx43↓(1)+eGFP fetal AM hMSCs (A2) did not. (A3) Punctate Cx45 immunostaining of the interface between a Cx43↓(1)+Cx45↑ fetal AM hMSC and an adjacent nrCMC (white arrows). (B) Quantitative analysis of the cardiomyogenic differentiation capacity of Cx43↓(1)+Cx45↑ fetal AM hMSCs and of Cx43↓(1)+eGFP fetal AM hMSCs using immunopositivity for sarcomeric α-actinin as read-out. The graph is based on a minimum of 5,000 cells analyzed from 4 separate hMSC isolates per experimental group. ND is not detected. (C1) Current-clamp recordings in pharmacologically uncoupled co-cultures of nrCMCs and Cx43↓(1)+eGFP fetal AM hMSCs or Cx43↓(1)+Cx45↑ fetal AM hMSCs. Fetal AM hMSCs that had lost the capacity to produce action potentials due to knockdown of Cx43 expression regained this ability following forced Cx45 expression but not after eGFP overexpression. (C2) Average MDPs of nrCMCs, Cx43↓(1)+eGFP fetal AM hMSCs and Cx43↓(1)+Cx45↑ fetal AM hMSCs. For the Cx43↓(1)+Cx45↑ fetal AM hMSCs, only the average MDP of cells showing action potentials is presented.

ASSESSMENT OF CARDIOMYOGENIC DIFFERENTIATION ABILITY OF FETAL AM HMSCS AFTER RESCUE OF CX43 KNOCKDOWN BY CX45 OVEREXPRESSION

Human-specific immunocytological evaluation

Ten days after co-incubation with nrCMCs, Cx43↓(1)+Cx45↑ fetal AM hMSCs and Cx43↓(1)+eGFP fetal AM hMSCs were analyzed for α-actinin positivity. While Cx43↓(1)+eGFP fetal AM hMSCs did not contain detectable amounts of α-actinin, 1.57±0.4% (n=2,500) GFP/human lamin A/C-double-positive Cx43↓(1)+Cx45↑ fetal AM hMSCs stained positive for this sarcomeric protein indicating that these human cells had differentiated into CMCs (Figure 7A1-A2 and B). Furthermore, only in co-cultures of Cx43↓(1)+Cx45↑ fetal AM hMSCs with nrCMCs, GFP-positive cells were detected that were positive for the cardiac transcription factors Nkx2.5 and GATA4 (Supplemental figure 4A1-B1). Cx43↓(1)+eGFP fetal AM hMSCs in co-culture with nrCMCs did not stain positive for these transcription factors (Supplemental figure 4A2-4B2).

hMSC-specific intracellular electrophysiological measurements

To further study the cardiomyogenic differentiation capacity of Cx43↓(1)+Cx45↑ fetal AM hMSCs, these cells were subjected to whole-cell current-clamp measurements following pharmacological uncoupling. Cx43↓(1)+eGFP fetal AM hMSCs (n=5) showed steady membrane potentials, while some of the Cx43↓(1)+Cx45↑ fetal AM hMSCs (n=5) produced spontaneous action potentials with MDPs comparable to those of nrCMCs (n=7) (-65±4 mV and -69±5 mV, respectively) (Figure 7C1-C2). Thus, the loss of excitability in Cx43↓(1) fetal AM hMSCs could be overcome by Cx45 overexpression, at least in a subpopulation of cells.

DISCUSSION

The key findings of this study are 1) Fetal hMSCs, which intrinsically express Cx43 at high levels, efficiently communicate with adjacent nrCMCs via gap junctions and can differentiate into functional heart muscle cells when co-cultured with nrCMCs. 2) Adult hMSCs that contain low amounts of Cx43 by nature do not undergo cardiomyogenic differentiation in co-culture with nrCMCs. 3) Overexpression of Cx43 in adult hMSCs does not lead to their cardiomyogenic differentiation upon co-culture with nrCMCs. 4) Cardiomyogenic differentiation of fetal hMSCs in co-culture with nrCMCs is inhibited by Cx43 knockdown, but is rescued by concurrent overexpression of Cx45.

GAP JUNCTIONS AND HMSCS

The expression of the three major cardiac Cx (i.e. Cx40, Cx43 and Cx45) genes by hMSCs has previously been demonstrated.[22,23] Also, the formation of functional gap junctions, important for integration of donor cells with the surrounding myocardium after cardiac stem cell therapy, has been shown to occur.[9,22,23] Recently, our group showed that hMSCs derived from fetal tissues contain much higher levels of Cx43 than those derived from adult tissues.[19] In addition, evidence was provided that hMSCs of embryonic or fetal origin can undergo cardiomyogenesis when co-cultured with nrCMCs while hMSCs derived from adult sources fail to do so. To directly investigate the role of gap junctional coupling in cardiomyogenic differentiation of hMSCs, in the present study, Cx43 expression was downregulated in fetal AM hMSCs and upregulated in adult AT hMSCs through LV gene transfer. These genetic interventions resulted in a strong reduction in gap junctional communication between fetal AM hMSCs and nrCMCs and led to a substantial increase in the gap junctional coupling between adult AT hMSCs and nrCMCs. In addition, it was investigated whether the effects of Cx43 knockdown could be reversed by Cx45 overexpression. The reason to choose Cx45 for this purpose was that it can be engaged in the formation of functional homotypic as well as heterotypic gap junctions composed of homomeric or heteromeric connexins.[24-27] In the current study, it was indeed established that after transduction with a Cx45-encoding LV, Cx43↓(1) fetal AM hMSCs express high levels of Cx45 mRNA leading to rescue of their efficient gap junctional communication with nrCMCs.

ROLE OF GAP JUNCTIONAL COMMUNICATION IN CARDIOMYOGENIC DIFFERENTIATION

Connexins have been reported to be involved in differentiation processes such as osteogenesis, neural differentiation and hematopoiesis.[28-32] However, little is known about the role of gap junctional communication in cardiomyogenic differentiation. As already stated above, our group recently found that fetal AM hMSCs express Cx43 at high levels in contrast to adult AT hMSCs. Interestingly, these fetal AM hMSCs were able to differentiate, in co-culture with nrCMCs, into functional CMCs while adult AT hMSCs were not.[19] Other investigators using co-cultures with CMCs to induce cardiomyogenic differentiation in stem cells have also proposed that intercellular communication through gap junctions might be essential in this differentiation process.[33,34] However, the role of gap junctional communication in the transfer of cardiomyogenic signals from CMCs to other cell types has not yet been investigated. In the current study, the role of Cx43 in cardiomyogenic differentiation of hMSCs in the presence of neighboring CMCs was further elucidated. Fetal AM hMSCs lost their ability to differentiate into functional CMCs after knockdown of Cx43 gene expression. However, not only did overexpression of Cx45 restore the ability of these hMSCs to form functional gap junctions with nrCMCs but it also

rescued the cardiomyogenic differentiation capacity of these fetal hMSCs upon co-incubation with nrCMCs. In contrast to these findings, adult AT hMSCs did not gain the ability to differentiate into functional CMCs after overexpression of Cx43. The inability of adult AT hMSCs to undergo cardiomyogenesis following co-culture with nrCMCs could have an epigenetic explanation.[35-37] According to this hypothesis, genes important for cardiomyogenic differentiation could, in adult AT hMSCs, exist in a transcriptionally repressive state imposed by specific DNA methylation patterns and/or chromatin signatures. Also, qualitative and/or quantitative differences in the repertoire of transcription factors and miRs expressed by fetal AM hMSCs and by adult AT hMSCs might contribute to their differential responsiveness to cardiomyogenic signals produced by neighboring nrCMCs.[38,39]

Since gap junctions enable intercellular communication, induction of cardiomyogenesis after co-incubation with nrCMCs may be caused by exchange of signals between nrCMCs and fetal hMSCs. Stimulation of cardiomyogenic differentiation by miRs-499, as previously described, has been inferred to be a gap junction-mediated process.[11] Moreover, intercellular communication makes [Ca^{2+}] oscillations possible, which has been shown to increase the regenerative potential of human cardiac progenitor cells in a mouse myocardial infarction model.[40] In line with these findings are the observations by Muller-Borer et al. who found that in co-culture with nrCMCs rat liver stem cells obtain CMC-like properties and display [Ca^{2+}] oscillations synchronous with those of adjoining CMCs. The [Ca^{2+}] oscillations in the liver stem cells were dependent on gap junctional communication with neighboring CMCs and their inhibition led to a decrease in the expression of CMC-specific genes by the liver stem cells.[34] The recent observation that hyperpolarization is sufficient to induce cardiomyogenic differentiation of human CMC progenitor cells underlines the importance of gap junctional coupling in this process.[12] In the current study, fetal AM hMSCs in co-culture with nrCMCs were hyperpolarized in contrast to those that were transduced with hCx43-specific shRNAs. More importantly, Cx43↓(1) fetal AM hMSCs were also hyperpolarized in co-culture with nrCMCs after overexpression of Cx45. As a matter of fact, the average MDPs of control fetal AM hMSCs and Cx43↓(1)+Cx45↑ fetal AM hMSCs in contact with nrCMCs were identical. This could explain why knockdown of Cx43 leads to an inability of fetal AM hMSCs to differentiate towards functional CMCs, while after subsequent Cx45 overexpression their cardiomyogenic differentiation potential was restored. So while the precise composition of the gap junctions involved in the restoration of the cardiomyogenic differentiation capacity in Cx43↓(1) fetal hMSCs following Cx45 overexpression remains elusive, the factor(s) that exert their cardiomyogenic effects on fetal AM hMSCs via gap junctions can pass Cx45-containing channels in high enough amounts to set off the cardiomyogenic differentiation of these cells.

CONCLUSIONS

The results of this study indicate that efficient gap junctional coupling with adjacent CMCs is essential to induce cardiomyogenic differentiation of naturally Cx43-rich fetal hMSCs in co-culture with nrCMCs. However, adult AT hMSCs that contain relatively low intrinsic levels of Cx43 and do not undergo cardiomyogenesis in the presence of nrCMCs, cannot be endowed with cardiomyogenic differentiation ability by overexpression of Cx43.

LIMITATION

It would have been of interest to conduct Cx43 knockdown experiments using a cell type with a higher propensity to differentiate into functional CMCs than fetal hMSCs. However, such a cell type was not available to us. Furthermore, it would have been clinically more relevant to co-culture different hMSC subtypes with adult human CMCs, but obtaining these cells in the numbers needed to conduct these experiments was impossible. Also, adult human CMCs cannot be maintained ex vivo long enough in a differentiated state to perform some of the key experiments described in this paper.

FUNDING

This research forms part of Project P1.04 SMARTCARE of the BioMedical Materials (BMM) program, which is co-funded by the Dutch Ministry of Economic Affairs, Agriculture and Innovation. The financial contribution of the Dutch Heart Foundation (NHS) is gratefully acknowledged. D.E.A. is funded by the Smart Mix Program of the Netherlands Ministry of Economic Affairs and the Netherlands Ministry of Education, Culture and Science. D.A.P. is recipient of Veni grant 91611070 from the Netherlands Organisation for Scientific Research (NWO).

REFERENCES

1. Maeda S, Tsukihara T. Structure of the gap junction channel and its implications for its biological functions. Cell Mol Life Sci 2011;68:1115-1129.
2. Levin M. Gap junctional communication in morphogenesis. Prog Biophys Mol Biol 2007;94:186-206.
3. Kumai M, Nishii K, Nakamura K et al. Loss of connexin45 causes a cushion defect in early cardiogenesis. Development 2000;127:3501-3512.
4. Reaume AG, de Sousa PA, Kulkarni S et al. Cardiac malformation in neonatal mice lacking connexin43. Science 1995;267:1831-1834.
5. Kirchhoff S, Kim JS, Hagendorff A et al. Abnormal cardiac conduction and morphogenesis in connexin40 and connexin43 double-deficient mice. Circ Res 2000;87:399-405.
6. Gu H, Smith FC, Taffet SM et al. High incidence of cardiac malformations in connexin40-deficient mice. Circ Res 2003;93:201-206.
7. Chi NC, Bussen M, Brand-Arzamendi K et al. Cardiac conduction is required to preserve cardiac chamber morphology. Proc Natl Acad Sci U S A 2010;107:14662-14667.
8. Abraham MR, Henrikson CA, Tung L et al. Antiarrhythmic engineering of skeletal myoblasts for cardiac transplantation. Circ Res 2005;97:159-167.
9. Roell W, Lewalter T, Sasse P et al. Engraftment of connexin 43-expressing cells prevents post-infarct arrhythmia. Nature 2007;450:819-824.
10. Coppen SR, Fukushima S, Shintani Y et al. A factor underlying late-phase arrhythmogenicity after cell therapy to the heart: global downregulation of connexin43 in the host myocardium after skeletal myoblast transplantation. Circulation 2008;118:S138-S144.
11. Hosoda T, Zheng H, Cabral-da-Silva M et al. Human cardiac stem cell differentiation is regulated by a mircrine mechanism. Circulation 2011;123:1287-1296.
12. van Vliet P, de Boer TP, van der Heyden MA et al. Hyperpolarization induces differentiation in human cardiomyocyte progenitor cells. Stem Cell Rev 2010;6:178-185.
13. Gerson SL. Mesenchymal stem cells: no longer second class marrow citizens. Nat Med 1999;5:262-264.
14. Prockop DJ. Marrow stromal cells as stem cells for nonhematopoietic tissues. Science 1997;276:71-74.
15. Choi YH, Kurtz A, Stamm C. Mesenchymal stem cells for cardiac cell therapy. Hum Gene Ther 2011;22:3-17.
16. Pijnappels DA, Schalij MJ, Atsma DE. Response to the letter by Rose et al. Circ Res 2009;104:e8.
17. Quevedo HC, Hatzistergos KE, Oskouei BN et al. Allogeneic mesenchymal stem cells restore cardiac function in chronic ischemic cardiomyopathy via trilineage differentiating capacity. Proc Natl Acad Sci U S A 2009;106:14022-14027.
18. Rose RA, Jiang H, Wang X et al. Bone marrow-derived mesenchymal stromal cells express cardiac-specific markers, retain the stromal phenotype, and do not become functional cardiomyocytes in vitro. Stem Cells 2008;26:2884-2892.
19. Ramkisoensing AA, Pijnappels DA, Askar SF et al. Human Embryonic and Fetal Mesenchymal Stem Cells Differentiate toward Three Different Cardiac Lineages in Contrast to Their Adult Counterparts. PLoS One 2011;6:e24164.
20. Pijnappels DA, Schalij MJ, Ramkisoensing AA et al. Forced alignment of mesenchymal stem cells undergoing cardiomyogenic differentiation affects functional integration with cardiomyocyte cultures. Circ Res 2008;103:167-176.
21. Swildens J, de Vries AA, Li Z et al. Integrin stimulation favors uptake of macromolecules by cardiomyocytes in vitro. Cell Physiol Biochem 2010;26:999-1010.

22. Valiunas V, Doronin S, Valiuniene L et al. Human mesenchymal stem cells make cardiac connexins and form functional gap junctions. J Physiol 2004;555:617-626.
23. Pijnappels DA, Schalij MJ, van Tuyn J et al. Progressive increase in conduction velocity across human mesenchymal stem cells is mediated by enhanced electrical coupling. Cardiovasc Res 2006;72:282-291.
24. Rackauskas M, Kreuzberg MM, Pranevicius M et al. Gating properties of heterotypic gap junction channels formed of connexins 40, 43, and 45. Biophys J 2007;92:1952-1965.
25. Schulte JS, Scheffler A, Rojas-Gomez D et al. Neonatal rat cardiomyocytes show characteristics of nonhomotypic gap junction channels. Cell Commun Adhes 2008;15:13-25.
26. Darrow BJ, Laing JG, Lampe PD et al. Expression of multiple connexins in cultured neonatal rat ventricular myocytes. Circ Res 1995;76:381-387.
27. Kwak BR, van Kempen MJ, Theveniau-Ruissy M et al. Connexin expression in cultured neonatal rat myocytes reflects the pattern of the intact ventricle. Cardiovasc Res 1999;44:370-380.
28. Yang SR, Cho SD, Ahn NS et al. Role of gap junctional intercellular communication (GJIC) through p38 and ERK1/2 pathway in the differentiation of rat neuronal stem cells. J Vet Med Sci 2005;67:291-294.
29. Montecino-Rodriguez E, Leathers H, Dorshkind K. Expression of connexin 43 (Cx43) is critical for normal hematopoiesis. Blood 2000;96:917-924.
30. Villars F, Guillotin B, Amedee T et al. Effect of HUVEC on human osteoprogenitor cell differentiation needs heterotypic gap junction communication. Am J Physiol Cell Physiol 2002;282:C775-C785.
31. Wong RC, Pera MF, Pebay A. Role of gap junctions in embryonic and somatic stem cells. Stem Cell Rev 2008;4:283-292.
32. Rossello RA, Wang Z, Kizana E et al. Connexin 43 as a signaling platform for increasing the volume and spatial distribution of regenerated tissue. Proc Natl Acad Sci U S A 2009;106:13219-13224.
33. Xu M, Wani M, Dai YS et al. Differentiation of bone marrow stromal cells into the cardiac phenotype requires intercellular communication with myocytes. Circulation 2004;110:2658-2665.
34. Muller-Borer BJ, Cascio WE, Esch GL et al. Mechanisms controlling the acquisition of a cardiac phenotype by liver stem cells. Proc Natl Acad Sci U S A 2007;104:3877-3882.
35. De Carvalho DD, You JS, Jones PA. DNA methylation and cellular reprogramming. Trends Cell Biol 2010;20:609-617.
36. Fisher CL, Fisher AG. Chromatin states in pluripotent, differentiated, and reprogrammed cells. Curr Opin Genet Dev 2011;21:140-146.
37. Goldberg AD, Allis CD, Bernstein E. Epigenetics: a landscape takes shape. Cell 2007;128:635-638.
38. Aranda P, Agirre X, Ballestar E et al. Epigenetic signatures associated with different levels of differentiation potential in human stem cells. PLoS One 2009;4:e7809.
39. Jansen BJ, Gilissen C, Roelofs H et al. Functional differences between mesenchymal stem cell populations are reflected by their transcriptome. Stem Cells Dev 2010;19:481-490.
40. Ferreira-Martins J, Rondon-Clavo C, Tugal D et al. Spontaneous calcium oscillations regulate human cardiac progenitor cell growth. Circ Res 2009;105:764-774.

SUPPLEMENTAL MATERIALS AND METHODS

ISOLATION, CULTURE AND CHARACTERIZATION OF HUMAN MESENCHYMAL STEM CELLS (HMSCS)

All investigations with human-derived tissues conformed to the Declaration of Helsinki and were approved by the Medical Ethics Committee of the Leiden University Medical Centre (LUMC). Written informed consent was obtained from all subjects or, in case of the fetal material, from the parents of the fetuses.

Human fetal amniotic membranes were collected from placentas at gestational weeks 17-22 through legal interventions by the Department of Obstetrics. The membranes were washed twice with phosphate-buffered saline (PBS) and finely minced into 1-2 mm fragments using scissors and scalpels. Cells were dissociated by treatment with 0.1% collagenase type I (Worthington, Lakewood, NJ) for 3 h at 37°C in a humidified 95% air/5% CO_2 atmosphere. Thereafter, 10 mL of Dulbecco's modified Eagle's medium (DMEM) containing 10% fetal bovine serum (FBS), 100 U/mL penicillin and 100 µg/mL streptomycin (all from Invitrogen, Breda, the Netherlands; hereinafter referred to as MSC medium) was added. The cell suspension was transferred to a 25-cm^2 culture flask (Becton Dickinson, Franklin Lakes, NJ) and incubated for 3-4 days at 37°C in a humidified atmosphere of 95% air/5% CO_2 to allow the cells to adhere. The MSC medium was replaced twice a week until the primary cultures had reached ±80% confluency, after which the fetal amniotic membrane (AM) hMSCs were amplified by serial passage using a buffered 0.05% trypsin-0.02% EDTA solution (TE; Lonza Vervier, Vervier, Belgium) for cell detachment.

Adult adipose tissue (AT) hMSCs were derived from subcutaneous abdominal fat tissue (n=4 donors, mean donor age 42.5±5.4 yrs). Tissue samples were washed twice with PBS containing 100 U/mL penicillin and 100 µg/mL streptomycin and finely minced with a scissor. For tissue disruption 0.1% collagenase type I solution was added and the samples were incubated for 1 h at 37°C in a humidified incubator containing 95% air and 5% CO_2. Collagenase type I activity was quenched by adding MSC medium. Samples were then centrifuged at 330×*g* for 10 min. After centrifugation the top layer of primary adipocytes was removed and the collagenase type I-containing solution was aspirated. The cell pellet was suspended in MSC medium, passed through a nylon cell strainer with a mesh pore size of 70 µm (Becton Dickinson) and the cells were once again collected by centrifugation. The latter procedure was repeated twice, after which the cell pellet was resuspended in 8 ml MSC medium. The resulting cell suspension was transferred to a 75-cm^2 culture flask (Becton Dickinson) and the adult AT hMSCs were expanded by serial passage using standard methods.

The isolated cells were characterized according to generally accepted criteria using flow cytometry for the detection of surface antigens and adipogenic and osteogenic differentiation assays to establish multipotency. Surface marker expression was examined after culturing the cells for at least 3 passages. Thereafter, the hMSCs were detached using TE, suspended in PBS containing 1% bovine serum albumin fraction V (BSA; Sigma-Aldrich Chemie, Zwijndrecht, the Netherlands) and divided in aliquots of 10^5 cells. Cells were then incubated for 30 min at 4°C with fluorescein isothiocyanate- or phycoerythrin-conjugated monoclonal antibodies (MAbs) directed against human CD105 (Ancell, Bayport, MN), CD90, CD73, CD45, CD34 or CD31 (all from Becton Dickinson). Labeled cells were washed three times with PBS containing 1% BSA and analyzed using a BD LSR II flow cytometer (Becton Dickinson). Isotype-matched control MAbs (Becton Dickinson) were used to determine background fluorescence. At least 10^4 cells per sample were acquired and data were processed using FACSDiva software (Becton Dickinson).

Established differentiation assays were used to determine the adipogenic and osteogenic differentiation ability of the cells.[1] Briefly, 5×10^3 hMSCs per well were plated in a 12-well culture plate (Corning Life Sciences, Amsterdam, the Netherlands) and exposed to adipogenic or osteogenic differentiation medium. Adipogenic differentiation medium consisted of MEM-plus (i.e. α-minimum essential medium [Invitrogen] containing 10% FBS, 100 U/mL penicillin and 100 µg/mL streptomycin) supplemented with insulin, dexamethason, indomethacin and 3-isobutyl-1-methylxanthine (all from Sigma-Aldrich Chemie) to final concentrations of 5 µg/mL, 1 µM, 50 µmol/L and 0.5 µmol/L, respectively, and was refreshed every 3-4 days for a period of 3 weeks. Lipid accumulation was assessed by Oil Red O (Sigma-Aldrich Chemie) staining of the cultures (15 mg of Oil Red O per mL of 60% 2-propanol). Osteogenic differentiation medium consisted of MEM-plus containing 10 mmol/L b-glycerophosphate, 50 µg/mL ascorbic acid and 10 nmol/L dexamethason (all from Sigma-Aldrich Chemie) and was refreshed every 3-4 days for a period of 3 weeks. Afterwards, the cells were washed with PBS and calcium deposits were visualized by staining of the cells for 5 min with 2% Alizarin Red S (Sigma-Aldrich Chemie) in 0.5% NH_4OH (pH 5.5).

ISOLATION AND CULTURE OF NEONATAL RAT CARDIOMYOCYTES AND CARDIAC FIBROBLASTS

All animal experiments were approved by the Animal Ethics Committee of the LUMC and conformed to the Guide for the Care and Use of Laboratory Animals, as stated by the US National Institutes of Health (permit number: 10236).[2]

Primary myocardial cells were dissociated from ventricles of 2-day-old male Wistar rats. Neonatal rat cardiomyocytes (nrCMCs) and cardiac fibroblasts (nrCFBs) were separated from each other by differential plating and maintained

in a 1:1 (v/v) mixture of DMEM and Ham's F-10 medium (MP Biomedicals, Solon, OH) containing 5% horse serum (Invitrogen), 100 U/mL penicillin and 100 µg/mL streptomycin as previously described.[3]

Myocardial cells were plated on fibronectin (Sigma-Aldrich Chemie)-coated coverslips (15 mm Ø) at a density of 2×10^5 cells per well in 12-well plates and incubated at 37°C in a humidified incubator containing 95% air and 5% CO_2. Proliferation of residual nrCFBs in nrCMC cultures was inhibited by incubating the cells with 10 mg/mL mitomycin-C (Sigma-Aldrich Chemie) in PBS for 1 h.[4]

Production of lentiviral vectors

Two self-inactivating (SIN) lentiviral vector (LV) shuttle plasmids encoding short hairpin (sh) RNAs targeting the human connexin 43 (hCx43) gene (i.e. TRCN0000059773 and TRCN0000059775) were selected from the Mission Library (Sigma-Aldrich Chemie). The shRNAs encoded by these constructs efficiently inhibit hCx43 expression in hMSCs as assessed by western blotting and contain sense strands that differ at 3 positions from the codinq sequence of the rat Cx43 gene. As negative control, a SIN-LV shuttle plasmid directing the synthesis of an enhanced green fluorescent protein (eGFP) gene-specific shRNA (SHC005; Sigma-Aldrich Chemie) was used. To allow for the easy assessment of transduction efficiencies, the puromycin N-acetyl transferase-coding sequence in each of these constructs was replaced by that of version I of the green fluorescent protein of *Renilla reniformis* (hrGFPI) as previously described.[5] The resulting SIN-LV shuttle plasmids were designated pLV.shRNA-hCx43.1.hPGK1.hrGFPI, pLV.shRNA-hCx43.2.hPGK1.hrGFPI and pLV.shRNA-eGFP.hPGK1.hrGFPI, respectively.

Overexpression of hCx43 or hCx45 in hMSCs was accomplished using bicistronic SIN-LVs. The shuttle plasmids for generating these SIN-LVs were made as follows. First, pIRES.hrGFPII (Stratagene/Agilent Technologies, Santa Clara, CA) was digested with HincII and XbaI and the 2.1-kb fragment containing the human cytomegalovirus immediate-early gene promoter, the internal ribosome entry site of encephalomyocarditis virus and the hrGFP version II open reading frame was combined with the 6.1-kb SmaI×XbaI fragment of pLV.MCS.WHVPRE (GenBank accession number: JN622008) to create pLV.hCMV-IE.IRES.hrGFPII.WHVPRE. Next, the hCx43- and hCx45-coding sequences were released from Mammalian Gene Collection clones IRATp970C0822D and IRAMp995E152Q (Source BioScience, LifeSciences, Nottingham, United Kingdom) by restriction enzyme digestion using EcoRI (hCx45) or CfrI and MunI (hCx43). After treatment with the Klenow fragment of DNA polymerase I, the resulting hCx43- and hCx45-coding fragments of 1.3 and 1.2 kb, respectively, were combined with the 8.3-kb Eco32I fragment of pLV.hCMV.IRES.hrGFPII.WHVPRE using T4 DNA ligase to create pLV.hCMV-IE.hCx43.IRES.hrGFPII.WHVPRE and pLV.hCMV-IE.hCx45.IRES.hrGFPII.WHVPRE.

As negative control the original SIN-LV shuttle plasmid pLV.hCMV-IE.IRES.hrGFPII.WHVPRE was used. All restriction and DNA modifying enzymes were obtained from Fermentas (St. Leon-Rot, Germany).

Ligation mixtures were introduced in chemocompetent GeneHogs cells (Invitrogen) and large stocks of the correct plasmids were prepared with the aid of the JETSTAR 2.0. Plasmid Maxiprep Kit (Genomed, Löhne, Germany).

Vesicular stomatitis virus G-protein-pseudotyped SIN human immunodeficiency virus type I vectors were produced in 175-cm^2 culture flasks (Greiner Bio-One, Alphen a/d Rijn, the Netherlands) seeded with 10^5 293T cells per cm^2 in DMEM supplemented with 10% FBS and 0.01 mmol/L cholesterol. The next day, the producer cells in each flask were transfected with a total of 35 µg of DNA at a 2:1:1 molar ratio of 1) one of the SIN-LV shuttle plasmids, 2) psPAX2 (Addgene, Cambridge, MA) and 3) pLP/VSVG (Invitrogen) using 3 µg of polyethyleneimine (Polysciences Europe, Eppelheim, Germany) per µg of DNA as transfection agent. Sixteen hours later, the transfection medium in each flask was replaced by 15 ml of DMEM containing 5% FBS, 10 mmol/L HEPES-NaOH (pH 7.4) and 0.01 mmol/L cholesterol. At 64 h post-transfection, the culture fluid was collected and freed of cellular debris by centrifugation at room temperature for 10 min at 825×*g* and filtration through a 0.45-µm pore-size cellulose acetate filter (Pall Corporation, East Hills, NY). To concentrate the SIN-LV particles, 5 ml of 20% (w/v) sucrose in PBS was carefully layered under 30 ml of the cleared culture medium, which was then centrifuged for 2 h at 15,000 rounds per min and 10°C in an SW28 rotor (Beckman Coulter, Fullerton, CA). Next, the supernatant was discarded and the pellet containing the SIN-LV particles was suspended in 500 µl of PBS-1% BSA by gentle rocking overnight at 4°C.

The gene transfer activity of the SIN-LV stocks was determined by end-point titration on HeLa indicator cells using flow cytometric analysis of hrGFPI or hrGFPII expression as read-out. The titers of the SIN-LV preparations are thus expressed in HeLa cell-transducing units (HTUs) per ml.

Overexpression of hCx43 was also established by a SIN-LV shuttle plasmid pLV.hCMV-IE.hCx43.IRES.PurR.hHBVPRE. This SIN-LV shuttle plasmid was constructed using a PCR-based cloning procedure. The hCx43-coding sequence was amplified by high-fidelity PCR from pLV.hCMV-IE.hCx43.IRES.hrGFPII.WHVPRE in 30 cycles using the primers 5' atacgcgttaacatgggtgactggagc 3' and 5' cgtgtacagttaacttagatctccaggtcatcagg 3' (Eurofins MWG Operon, Ebersberg, Germany), Bioline's VELOCITY DNA polymerase (GC biotech, Alphen aan den Rijn, the Netherlands) and the standard reaction conditions, including an annealing temperature of 55°C, recommended by the supplier. The 1175-bp PCR product was purified using Sure-Clean (Bioline), incubated with the restriction enzymes MluI and Bsp1407I (both from Fermentas) and the 1.2-kb digestion product was extracted from agarose gel

using JetSorb Gel Extraction Kit (GENOMED). Finally, the hCx43-coding DNA fragment was combined with the 8.2-kb MluI× Bsp1407I fragment of pLV.CMV.IRES.PURO[6] to generate pLV.hCMV-IE.hCx43.IRES.PurR.hHBVPRE. This SIN-LV shuttle plasmid was subsequently used for the production of SIN-LV vector particles as described above.

TRANSDUCTION OF HMSCS

hMSCs were seeded at a density of 2×10^4 cells per well in 6-well plates (Corning) and incubated overnight in a humidified 95% air/5% CO_2 atmosphere. Next, the culture fluid was replaced by 1 ml per well of fresh MSC medium supplemented with 10 µg/ml diethylaminoethyl-dextran sulfate (GE Healthcare, Leiderdorp, the Netherlands) and 20 HTUs per cell of SIN-LV. After an incubation period of 4 h at 37°C in a humidified atmosphere of 5% CO_2 in air, the cells were washed with PBS, cultured in MSC medium and passaged ≥2 times before being used in any of the co-culture experiments. AT hMSCs were transduced with LV.hCMV-IE.hCx43.IRES.hrGFPII.WHVPRE or pLV.hCMV-IE.hCx43.IRES.PurR.hHBVPRE to overexpress Cx43 (Cx43↑ adult AT hMSCs), while cells exposed to LV.hCMV-IE.IRES.hrGFPII.WHVPRE or pLV.CMV.IRES.PURO served as control (control adult AT hMSCs). Adult AT hMSCs transduced with LVs encoding for the puromycin-resistence gene, were cultured in MSC medium supplemented with 5 ug/mL puromycin (Sigma-Aldrich) for at least three weeks before any of the following experiments were conducted. To suppress hCx43 gene expression, fetal AM hMSCs were transduced with LV.shRNA-hCx43.1.hPGK1.hrGFPI (Cx43↓[1] fetal AM hMSCs) or with LV.shRNA-hCx43.2.hPGK1.hrGFPI (Cx43↓[2] fetal AM hMSCs). Fetal AM hMSCs used as control cells (control fetal AM hMSCs) were incubated with LV.shRNA-eGFP.hPGK1.hrGFPI. Cx43↓(1) fetal AM hMSCs were transduced with LV.hCMV-IE.hCx45.IRES.hrGFPII.WHVPRE to overexpress Cx45 (Cx43↓(1)+Cx45↑ fetal AM hMSCs) in these cells. Cx43↓(1) fetal AM hMSCs transduced with the eGFP-encoding SIN-LV LV.hCMV-IE.IRES.eGFP.HBVPRE (previously designated LV-CMV-IRES-eGFP[7]) were used as control cells (Cx43↓(1)+eGFP fetal AM hMSCs).

ANALYSIS OF CX43 AND CX45 EXPRESSION

The distribution of Cx43 and Cx45 was studied by immunocytological stainings as described previously.[8] In short, cells were fixed on ice with 4% paraformaldehyde in PBS for 30 min, washed with PBS, permeabilized with 0.1% Triton X-100 in PBS for 5 min at 4°C and rinsed again with PBS. To decrease non-specific binding of the primary antibodies the cells were incubated with 1% donkey serum (Sigma Aldrich Chemie) in PBS for 30 min. Thereafter, cells were incubated overnight at 4°C with Cx43-specific rabbit polyclonal antibodies (PAbs; C6219; Sigma Aldrich Chemie) or with Cx45-specific goat PAbs (C-19; Santa Cruz Biotechnology, Santa Cruz, CA)

diluted 1:200 and 1:100, respectively, in PBS containing 0.1% donkey serum. Binding of these primary antibodies to their target antigen was visualized using Alexa 568-conjugated donkey anti-rabbit IgG or anti-goat IgG (both from Invitrogen) at dilutions of 1:200. Nuclei were stained by incubating the cells for 10 min at room temperature with 10 μg/mL Hoechst 33342 (Invitrogen) in PBS. Cells that went through the entire staining procedure but were not exposed to primary antibodies served as negative controls. A fluorescence microscope equipped with a digital color camera (Nikon Eclipse 80i; Nikon Europe, Badhoevedorp, the Netherlands) and dedicated software (NIS Elements, Nikon) were used to analyze the data.

Quantification of Cx43 and Cx45 protein levels was done by western blot analysis. Lysates were made from $^{3}4$ different isolates of hMSCs per experimental group. After determining the protein concentration in each sample using the BCA Protein Assay Reagent (Thermo Fisher Scientific, Etten-Leur, the Netherlands), equal amounts of protein per slot was size-fractionated in a 12% NuPage Bis-Tris gel (Invitrogen) and transferred to a Hybond-P polyvinylidene difluoride membrane (GE Healthcare) using a wet blotting system. This membrane was blocked for 1 h at room temperature with 2% blocking buffer (ECL Advance blocking agent; GE Healthcare) in Tris-buffered saline wit Tween-20 (TBST) solution composed of 10 mmol/L Tris-HCl (pH7.6), 0.05% Tween-20 and 150 mmol/L NaCl. Thereafter, the membrane was incubated for 1 h at room temperature with the PAbs directed against Cx43 or Cx45 diluted 1:15,000 and 1:2,000 in blocking buffer, respectively. After multiple washing steps in TBST, the membrane was incubated with horseradish peroxidase (HRP)-conjugated goat anti-rabbit or donkey anti-goat secondary antibodies (both from Santa Cruz Biotechnology) diluted 1:15,000. For normalization purposes, a mouse MAb recognizing the housekeeping protein glyceraldehyde-3-phosphate dehydrogenase (GAPDH; Chemicon International, Temecula, CA; clone 6C5) was used, which was detected by HRP-conjugated goat anti-mouse secondary antibodies (Santa Cruz Biotechnology; 1:15,000). Chemiluminescence was induced with the aid of the ECL Advance Western Blotting Detection Kit and was captured on Hyperfilm ECL (both from GE Healthcare). The intensity of the Cx43-, Cx45- and GAPDH-specific signals was quantified using Image J software (version 1.43; National Institutes of Health, Bethesda, MD). For each sample, the ratios between the GAPDH signal intensity and that of the Cx43 or Cx45 protein were taken as measure of the absolute amounts of both these gap junction proteins in the different hMSC cultures. The Cx43 or Cx45 levels in the experimental samples were expressed as percentage of those of the corresponding control samples, which were set to 100%.

hCx43 and hCx45 transcript levels were determined by quantitative reverse transcription-polymerase chain reaction (qRT-PCR). To this purpose, total cellular RNA was extracted from $^{3}4$ samples for each group of hMSCs using the RNeasy Mini

Kit (QIAGEN Benelux, Venlo, the Netherlands). cDNA was synthesized in 20-µl volumes using 2 µg of RNA, 0.25 µg of random hexanucleotides, 25 nmol of dNTPs and 500 U of Superscript III RNase H^- reverse transcriptase (all from Invitrogen). The resultant cDNA was amplified by PCR using the primer pairs QT00012684 and QT00239659 (both from QIAGEN), which are specific for the hCx43 (official name: human gap junction protein, alpha 1 [GJA1]) and hCx45 (official name: human gap junction protein, gamma 1 [GJC1]) gene, respectively. The annealing temperature for these primer combinations was 55°C. The expression of the genes of interest was normalized to that of the housekeeping gene GAPDH using primer set QT01192646 (QIAGEN) also at an annealing temperature of 55°C. The resultant cDNA was PCR amplified using the QuantiTect SYBR Green PCR kit (QIAGEN) following the recommendations of the supplier. Agarose gel electrophoresis and melting curve analysis were carried out to verify that each primer pair yielded a single PCR product of the expected size. PCR amplifications carried out with human right atrium-specific cDNA or without cDNA served as positive and negative controls, respectively. Data were analyzed using the ΔCt method.[9]

ASSESSMENT OF FUNCTIONAL HETEROCELLULAR GAP JUNCTIONAL

Dye transfer

Dye transfer assays were used to directly determine functional heterocellular coupling between nrCMCs and the GFP-positive hMSCs. Four days after cell isolation, nrCMC cultures with a density of 2×10^5 cells per 3.8-cm^2 well were loaded with dye by incubation for 15 min with 4 mmol/L calcein red-orange AM (calcein; Invitrogen) in Hank's balanced salt solution (Invitrogen). Thereafter, the cells were rinsed three times with PBS and were kept in the incubator in nrCMC culture medium supplemented with 2.5 mmol/L probenecid (Invitrogen) for ^{3}30 min before 2×10^4 GFP-positive hMSCs were added. Fluorescent images (^{3}30 per group) were captured after 10 h and evaluated in a blinded manner. In all experimental groups, GFP-positive hMSCs surrounded by the same number of nrCMCs were analyzed. ImageJ software was used to determine the intensity of the calcein-associated fluorescence in several randomly-chosen, equally-sized subcellular regions for both the GFP-positive hMSCs and the adjoining nrCMCs. To correct for possible variations in calcein loading efficiency, the dye intensity in the GFP-positive hMSCs was expressed as a percentage of that in the surrounding nrCMCs. The percentage of calcein-positive cells among the GFP-labeled hMSCs was also determined by counting these cells in ^{3}60 fields of view per group.

Intracellular measurements

Whole-cell patch-clamp measurements were performed in co-cultures of 2×10^6 nrCMCs and 5×10^4 GFP-positive hMSCs. Typically, 4-6 nrCMCs were adjacent to a single hMSC. Four days after culture initiation, current-clamp recordings were performed at 25°C using an L/M-PC patch-clamp amplifier (List-Medical, Darmstadt, Germany; 3 kHz filtering).[8] Tip and seal resistance were 2.0-2.5 MW and >1 GW, respectively. The pipette solution contained (in mmol/L) 10 Na_2ATP, 115 KCl, 1 $MgCl_2$, 5 EGTA and 10 HEPES/KOH (pH 7.4) and the bath solution consisted of (in mmol/L) 137 NaCl, 4 KCl, 1.8 $CaCl_2$, 1 $MgCl_2$ and 10 HEPES (pH 7.4) in water. pClamp/Clampex8 software (Axon Instruments, Molecular Devices, Sunnyvale, CA) was used for data acquisition and analysis. All patch-clamp measurements were conducted in a blinded manner.

ASSESSMENT OF CARDIOMYOGENIC DIFFERENTIATION

To investigate their cardiomyogenic differentiation ability, 2×10^4 hMSCs from each experimental group were co-incubated for 10 days with 2×10^5 nrCMCs. The GFP-positive hMSCs were added to the nrCMC cultures 2 days after isolation of the nrCMCs.

Human-specific immunocytological analysis of cardiomyogenic differentiation potential

Immunocytological stainings were conducted as previously described.[3] On day 10 after culture initiation, the co-cultures of nrCMCs and GFP-positive hMSCs were fixed and stained with a mouse MAb recognizing the sarcomeric protein α-actinin (clone EA53; Sigma-Aldrich Chemie; dilution 1:400) and with the Cx43-specific PAb described above or in case of nrCMC co-cultures with Cx43↓(1)+Cx45↑ fetal AM hMSCs with a Cx45-specific PAb (clone H-85; Santa Cruz Biotechnology, dilution 1:200). The primary antibodies were visualized using Alexa 568-coupled donkey anti-mouse IgG and Alexa 532-linked goat anti-rabbit IgG secondary antibodies at dilutions of 1:200. Besides through their green fluorescence, the hMSCs in the co-cultures were identified by labeling with a human lamin A/C-specific murine MAb (clone 636; Vector Laboratories, Burlingame, CA; dilution 1:200). Lamin A/C staining was visualized with Qdot 655-streptavidin conjugates (Invitrogen; dilution 1:200) after incubation of the cells with biotinylated goat anti-mouse IgG2b secondary antibodies (Santa Cruz Biotechnology; dilution 1:200). Nuclei were stained using a 10 µg/mL solution of Hoechst 33342 in PBS. Co-cultures of nrCMCs with adult AT hMSCs transduced with LVs encoding for the puromycin-resistence gene instead of GFP were stained with primary Abs recognizing α-actinin, Cx43 and human-specific lamin A/C. The Cx43 PAb was visualized using an Alexa 488-coupled donkey anti-rabbit IgG, while α-actinin and human-specific lamin A/C

were visualized as described above. The percentage of GFP/lamin A/C-double-positive cells expressing α-actinin was determined by the microscopic analysis, at 40× magnification, of 25 cultures (200 cells per culture) of a total of 4 hMSC isolates per experimental group. Furthermore, the co-cultures were also stained with a goat PAb recognizing the cardiac transcription factor GATA4 (clone C-20; Santa Cruz Biotechnology, dilution 1:100) or with an Nkx2.5-specific rabbit PAb (clone H-114; Santa Cruz Biotechnology, dilution 1:200). These primary antibodies were visualized using Alexa 568-coupled donkey anti-goat or anti-rabbit IgG secondary antibodies (dilutions of 1:200). A fluorescence microscope equipped with a digital color camera (Nikon Eclipse 80i, Nikon Europe, Badhoevedorp, the Netherlands) and dedicated software (NIS Elements, Nikon) were used to analyze the data. All co-cultures were treated equally using the same antibody dilutions and exposure times.

Electrophysiological measurements in co-cultures of hMSCs and nrCMCs after pharmacological uncoupling

Cells were plated, cultured and studied under the same conditions as described above. Whole-cell current-clamp recordings were performed 10 days after culture initiation. Prior to the start of the measurements, the cells were treated for 15 min with 180 μmol/L of the pharmacological gap junctional uncoupler 2-aminoethoxydiphenyl borate (Tocris, Ballwin, MO) as previously described.[8] All measurements were conducted in a blinded manner.

STATISTICS

Experimental results were expressed as mean±standard deviation for a given number (n) of observations. Data was analyzed by Student's t-test for direct comparisons. Analysis of variance followed by appropriate *post-hoc* analysis was performed for multiple comparisons. Statistical analysis was carried out using SPSS 16.0 for Windows (SPSS, Chicago, IL). Differences were considered statistically significant at $P<0.05$.

REFERENCES

1. Pittenger MF, Mackay AM, Beck SC et al. Multilineage potential of adult human mesenchymal stem cells. Science 1999;284:143-147.
2. National Institutes of Health. Guide for the Care and Use of Laboratory Animals. 1-1-2002.
3. Pijnappels DA, Schalij MJ, van Tuyn J et al. Progressive increase in conduction velocity across human mesenchymal stem cells is mediated by enhanced electrical coupling. Cardiovasc Res 2006;72:282-291.
4. Askar SF, Ramkisoensing AA, Schalij MJ et al. Antiproliferative treatment of myofibroblasts prevents arrhythmias in vitro by limiting myofibroblast-induced depolarization. Cardiovasc Res 2011;90:295-304.
5. Swildens J, de Vries AA, Li Z et al. Integrin stimulation favors uptake of macromolecules by cardiomyocytes in vitro. Cell Physiol Biochem 2010;26:999-1010.
6. Uil TG, de VJ, Vellinga J et al. A lentiviral vector-based adenovirus fiber-pseudotyping approach for expedited functional assessment of candidate retargeted fibers. J Gene Med 2009;11:990-1004.
7. van Tuyn J, Pijnappels DA, de Vries AA et al. Fibroblasts from human postmyocardial infarction scars acquire properties of cardiomyocytes after transduction with a recombinant myocardin gene. FASEB J 2007;21:3369-3379.
8. Pijnappels DA, Schalij MJ, Ramkisoensing AA et al. Forced alignment of mesenchymal stem cells undergoing cardiomyogenic differentiation affects functional integration with cardiomyocyte cultures. Circ Res 2008;103:167-176.
9. Schefe JH, Lehmann KE, Buschmann IR et al. Quantitative real-time RT-PCR data analysis: current concepts and the novel "gene expression's CT difference" formula. J Mol Med (Berl) 2006;84:901-910.

SUPPLEMENTAL FIGURES

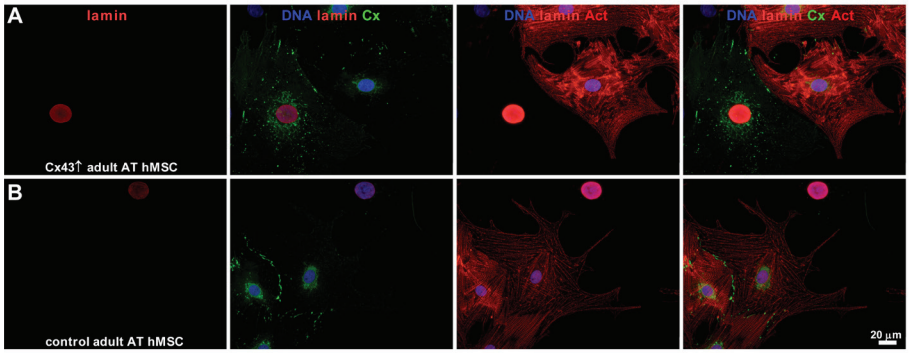

Supplemental Figure 1. Immunocytological assessment of cardiomyogenic differentiation of genetically modified adult AT hMSCs after 10 days of co-culture with nrCMCs. (A-B) Upon co-culture with nrCMCs, Cx43↑ adult AT hMSCs nor control adult AT hMSCs stained positive for α-actinin. Cx43 (indicated as Cx) plaques at the interfaces between Cx43↑ adult AT hMSCs and an adjacent nrCMC are present.

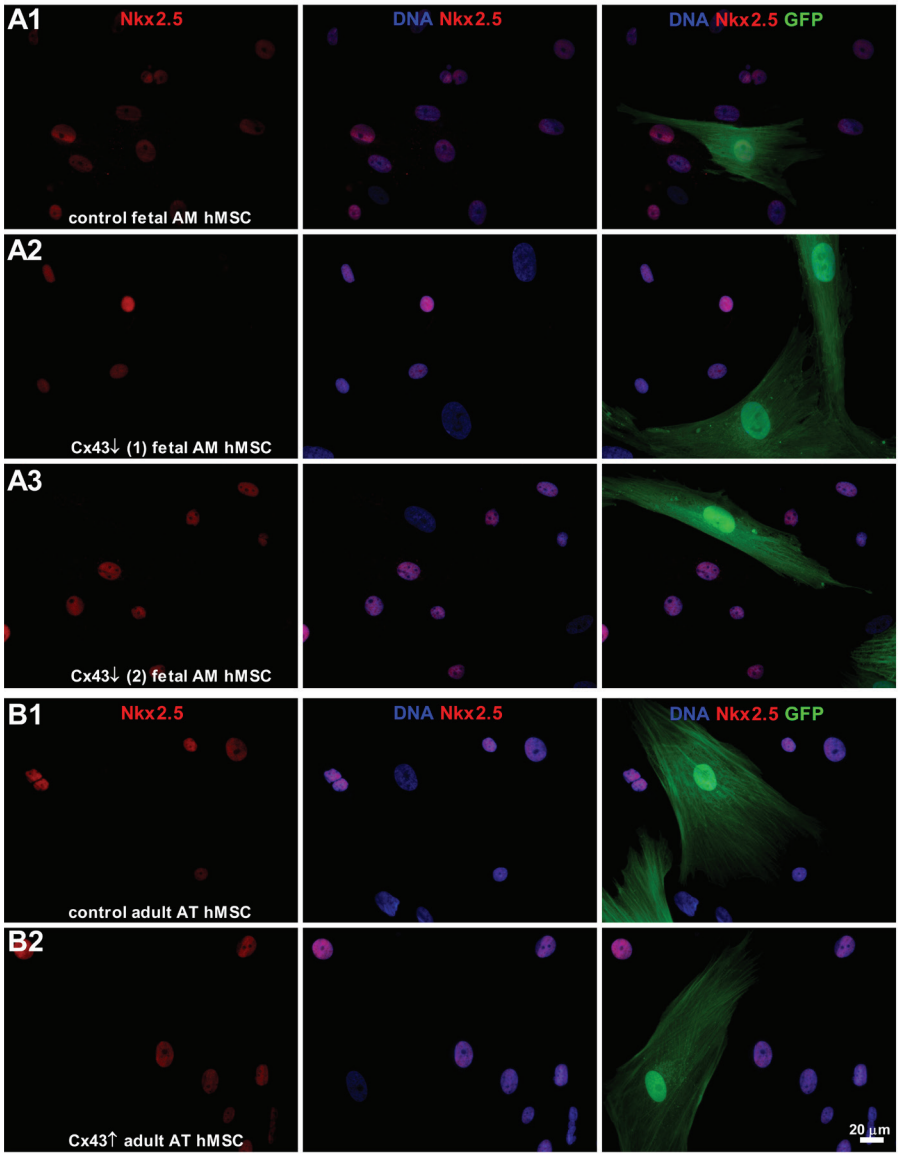

Supplemental figure 2. Immunocytological assessment of cardiomyogenic differentiation of genetically modified adult AT hMSCs and fetal AM hMSCs after 10 days of co-culture with nrCMCs. (A1) Upon co-culture with nrCMCs, a fraction of the GFP-positive control fetal AM hMSCs became positive for the cardiac transcription factor Nkx2.5. (A2-A3, B1-B2) GFP-labeled Cx43↓(1) fetal AM hMSCs, Cx43↓(2) fetal AM hMSCs, Cx43↑ adult AT hMSCs and control adult AT hMSCs in co-culture with nrCMCs did not stain positive for Nkx2.5.

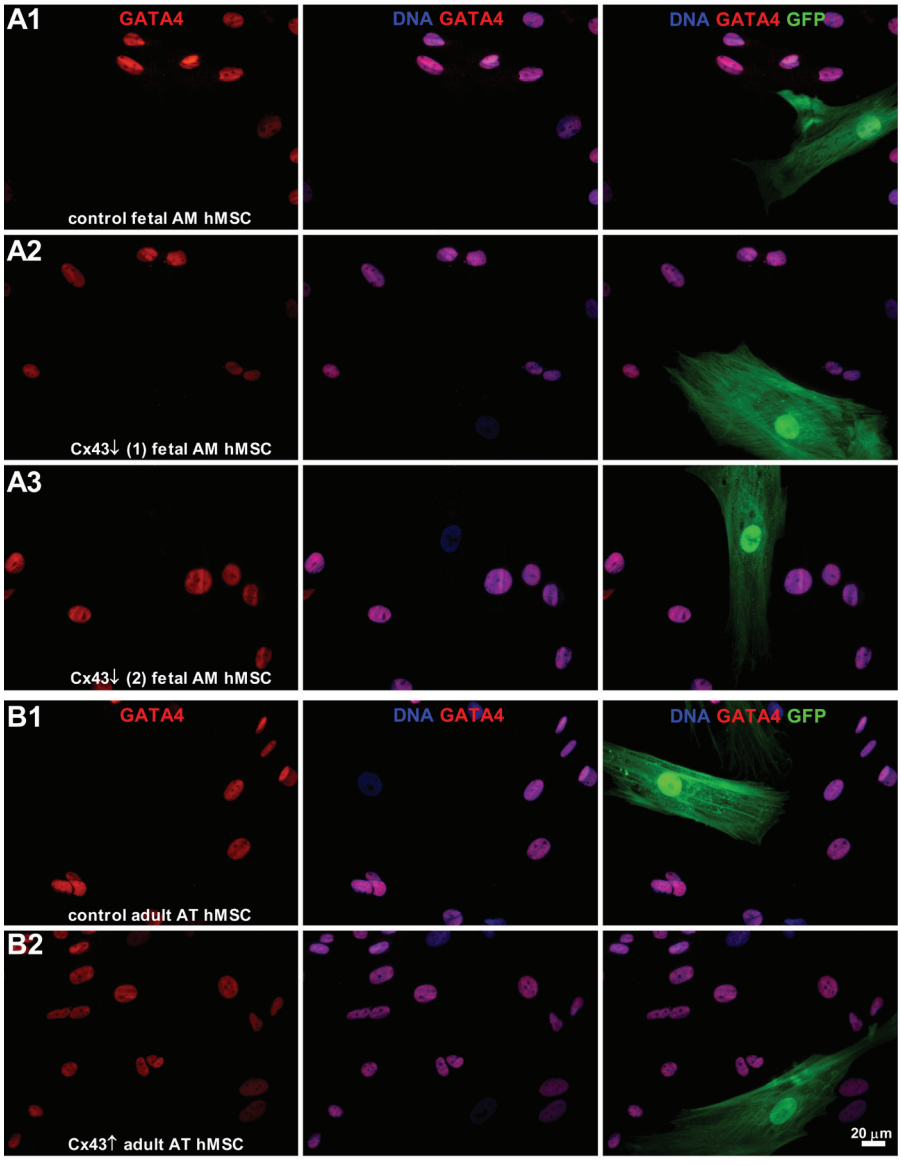

Supplemental figure 3. Immunocytological assessment of cardiomyogenic differentiation of genetically modified adult AT hMSCs and fetal AM hMSCs after 10 days of co-culture with nrCMCs. (A1) Upon co-culture with nrCMCs, a fraction of the GFP-positive control fetal AM hMSCs became positive for the cardiac transcription factor GATA4. (A2-A3, B1-B2) GFP-labeled Cx43↓ (1) fetal AM hMSCs, Cx43↓(2) fetal AM hMSCs, Cx43↑ adult AT hMSCs and control adult AT hMSCs in co-culture with nrCMCs did not stain positive for GATA4.

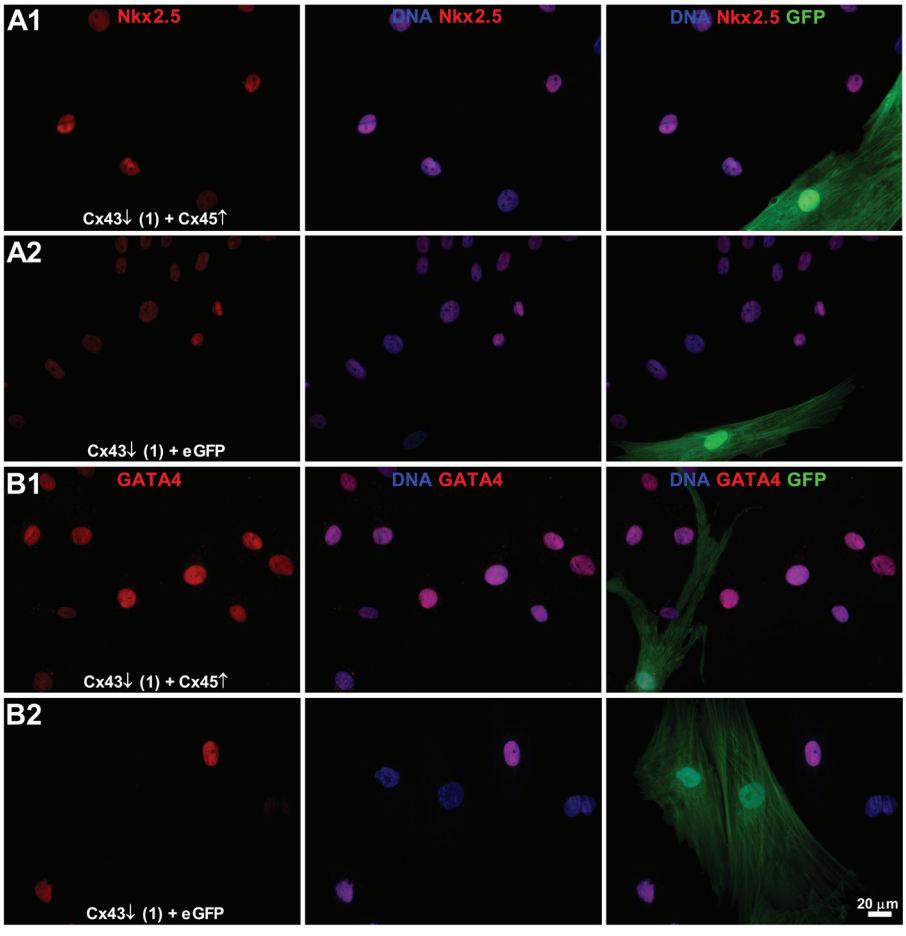

Supplemental figure 4. Investigation by immunocytology of cardiomyogenic differentiation of fetal AM hMSCs in co-culture with nrCMCs after rescue of Cx43 knockdown by Cx45 overexpression. In the presence of nrCMCs, a fraction of the GFP-positive Cx43↓(1)+Cx45↑ fetal AM hMSCs (A1 and B1) expressed Nkx2.5 and GATA4, while Cx43↓(1)+eGFP fetal AM hMSCs (A2 and B2) did not.